



ELSEVIER

Journal of Inorganic Biochemistry 81 (2000) 259–266

JOURNAL OF
**Inorganic
Biochemistry**

www.elsevier.nl/locate/jinorgbio

Ionic strength and pH effect on the Fe(III)-imidazolate bond in the heme pocket of horseradish peroxidase: an EPR and UV–visible combined approach

Enzo Laurenti^a, Gianpaolo Suriano^{a,b}, Elena M. Ghibaudi^a, Rosa Pia Ferrari^{a,*}^aDipartimento di Chimica I.F.M., Università di Torino, Via P. Giuria 7, 10125 Torino, Italy^bService de Genetique Appliquee, ULB-CRI, Rue des Profs Jeener et Brachet, 12 6041 Gosselies, Belgium

Received 4 January 2000; received in revised form 29 May 2000; accepted 19 June 2000

Abstract

The effects of chloride, dihydrogenphosphate and ionic strength on the spectroscopic properties of horseradish peroxidase in aqueous solution at pH=3.0 were investigated. A red-shift ($\lambda=408$ nm) of the Soret band was observed in the presence of 40 mM chloride; 500 mM dihydrogenphosphate or chloride brought about a blue shift of the same band ($\lambda=370$ nm). The EPR spectrum of the native enzyme at pH 3.0 was characterized by the presence of two additional absorption bands in the region around $g=6$, with respect to pH 6.5. Chloride addition resulted in the loss of these features and in a lower rhombicity of the signal. A unique EPR band at $g=6.0$ was obtained as a result of the interaction between HRP and dihydrogenphosphate, both in the absence and presence of 40 mM Cl^- . We suggest that a synergistic effect of low pH, Cl^- and ionic strength is responsible for dramatic modifications of the enzyme conformation consistent with the Fe(III)–His170 bond cleavage. Dihydrogenphosphate as well as high chloride concentrations are shown to display an unspecific effect, related to ionic strength. A mechanistic explanation for the acid transition of HRP, previously observed by Smulevich et al. [Biochemistry 36 (1997) 640] and interpreted as a pure pH effect, is proposed. © 2000 Elsevier Science S.A. All rights reserved.

Keywords: Horseradish peroxidase; Anion binding; Ionic strength; pH effect; Electron paramagnetic resonance spectroscopy

1. Introduction

Peroxidases form a widely distributed class of glycoenzymes, responsible for the oxidation of several organic and inorganic substrates. Their catalytic mechanism has been well-characterized [1–3] and implies the formation of two redox intermediates, called Compound I and Compound II. Compound I is a radical species ($\text{Fe(IV)=O-porphyrin}^+$) characterized by high oxidative power (it lies two oxidative equivalents above the resting state of the enzyme); Compound II is an oxo-ferryl species and it is still able to monoelectronically oxidize one substrate molecule.

Horseradish peroxidase is one of the most studied members of the plant peroxidase superfamily [3–9]. The X-ray structure of recombinant HRP isoenzyme C (rHRPc) (2.15 Å resolution) as well as that of its adduct with

benzhydroxamic acid (2.0 Å resolution) have been reported [10,11]. Two amino-acids, His42 and Arg38, have been identified as key-residues in the distal part of the heme pocket, by using site-directed mutagenesis [12–14]. These amino-acids are kept in all peroxidases that have been sequenced up-to-now and their position with respect to the heme was previously predicted by a theoretical structural model of HRP [15].

The X-ray structure has shown that His170 (which is the proximal histidine) is covalently bound to the iron ion and H-bonded to Asp247; this H-bond is crucial for stabilizing the iron in a five-coordinated geometry, as shown by both Raman Resonance measurements performed at neutral pH [12] and X-ray diffraction data [10]. H-bonding also affects the redox potential of the higher oxidation states of the enzyme, by modulating the basicity of the axial ligand [10,15]. A water molecule (Wat92) has been reported as lying at 3.2 Å from the iron and it is hydrogen-bonded to the $\text{N}\epsilon_2$ of Arg38 (3.0 Å), the $\text{N}\epsilon$ of His 42 (2.9 Å) and to a second water molecule (Wat123) [10]. In the rHRPc-benzhydroxamic acid adduct, Wat92 has been shown to coordinate the iron as the sixth axial ligand [11].

*Corresponding author. Tel.: +39-11-670-7516; fax: +39-11-670-7855.

E-mail address: ferrari@ch.unito.it (R.P. Ferrari).

Low temperature EPR measurements on native HRP showed a rhombic ferric high-spin signal, which was interpreted as a quantum-mechanical admixture of high-spin ($S=5/2$) and intermediate-spin ($S=3/2$) states [6].

HRP is known to contain two distinct Ca^{2+} -binding sites [10,16], one localized on the proximal side and the other on the distal side of the heme. Ca^{2+} is known to modulate both enzyme activity [16,17] and stability [18]. X-ray studies on HRP pointed out that both Ca^{2+} ions are hepta-coordinated. A complex hydrogen-bond network couples the Ca^{2+} -binding-sites on both sides of the heme: thus, the conformational structure of the HRP active site is highly sensitive to pH-changes or Ca^{2+} -depletion and, in general, to any perturbation of the H-bonds network [10]. This is consistent with previous observations on pH-driven transitions of HRP. Indeed, deprotonation of Arg38 was shown to be related to an alkaline transition occurring at pH 11.5 [19,20]. A conformational transition of HRP at pH 3.1 (in 500 mM phosphate buffer and 500 mM sodium chloride), possibly due to weakening or cleavage of the Fe-imidazolite bond, was observed as well and claimed as a pure pH effect [21].

We investigated the influence of chloride and dihydrogenphosphate on the conformation of HRP heme pocket at pH 3.0 in aqueous solution. A combined approach of EPR and UV–Visible absorption spectroscopy was used. Our data are consistent with the presence of a synergistic effect between chloride binding and ionic strength, which is critically dependent on low pH conditions.

2. Materials and methods

Horseshoe peroxidase cationic isoenzyme was purchased from Sigma Chem. Co. as lyophilized powder (type VI A, $\text{RZ}_{403/280}=3.2$). 4-Methylcatechol (Sigma), H_2O_2 (Merck) and all other reagents were of analytical grade. Enzyme solutions were made by first solubilizing HRP in distilled water and then adjusting the pH by addition of 2 M HCl; HRP concentration was determined from the Soret band absorbance (403 nm, $\epsilon=102 \text{ mM}^{-1} \text{ cm}^{-1}$). The desired ligand concentration was obtained by adding aqueous HRP solutions at pH 3.0 with proper amounts of NaCl or NaH_2PO_4 dissolved in water at pH 3.0. pH was checked before each measurement and adjusted to the desired value, when necessary.

Spectrophotometric measurements were performed by using a Kontron Uvikon930 double-beam spectrophotometer, with 10 mm-path length cells. Cells compartment was equipped with magnetic stirrer and a temperature control device. All optical measurements were recorded at 25°C, by using either quartz or PMMA/UV-grade cells (Kartell).

EPR studies were carried out on a Varian E109 X band spectrometer equipped with a Stellar AQM/Auriga XT data

system and an Oxford Instruments Cryostat (temperature range: 3.8–300 K).

2.1. Activity measurements

HRP activity measurements were performed on a series of samples by means of UV–Visible spectroscopy, following the oxidation of 4-methylcatechol to its quinone form ($\lambda_{\text{max}}=401 \text{ nm}$ and $\epsilon=1070 \text{ M}^{-1} \text{ cm}^{-1}$ [22]). Two millilitres of aqueous solution at pH 3.0, containing HRP (50 nM), 4-methylcatechol (0.75 mM), H_2PO_4^- (0–500 mM) and/or Cl^- (40–500 mM) were added with H_2O_2 up to a final concentration of 0.74 mM. Specific activity was expressed as $\mu\text{mol product min}^{-1} (\text{mg enzyme})^{-1}$.

2.2. UV–visible characterization and binding measurements

HRP UV–visible spectra were recorded at pH 3.0 (in water) and 6.5 (either in water or in 10 mM phosphate buffer) respectively; 2 ml of enzyme solution (5 μM) were employed. Thirty-minutes time-course measurements were carried out on enzyme solutions at pH 3.0 in the presence of 40 to 400 mM chloride and/or 400 mM dihydrogenphosphate, in order to monitor the evolution of their optical spectra.

Binding measurements were done by optical titration as previously reported [22,23]. Two ml enzyme solution (6–8 μM in water at pH 3.0) and 2 ml aqueous solution, in the sample and reference cell respectively, underwent subsequent additions of ligand aqueous solution at pH 3.0 up to a volume of 4.0 ml. The final ligand concentration was: 40 or 400 mM for Cl^- ; 400 mM for H_2PO_4^- , respectively. A spectrum was taken 5 min after each addition. Competitive binding measurements were carried out in the presence of 40 mM Cl^- , by adding increasing amounts of H_2PO_4^- (up to 400 mM).

2.3. EPR measurements

EPR spectra of HRP samples were recorded at pH 3.0 and 6.5 respectively. The enzyme was dissolved in water at pH 3.0 or pH 6.5 and in 10 mM phosphate buffer at pH 6.5, up to 0.1 mM concentration. EPR spectra of HRP aqueous solutions at pH 3.0 in the presence of: (a) 40 or 500 mM Cl^- , (b) 10–500 mM H_2PO_4^- and c) 40 mM Cl^- + 500 mM H_2PO_4^- were recorded. Two hundred microlitres samples were introduced in quartz EPR tubes (\varnothing 3 mm) and the Bruker strong pitch ($g=2.0029$) was employed as a standard in the reference cavity. All EPR spectra were recorded at 4 K with the following instrumental settings: 9.35 GHz microwave frequency, 100 KHz modulation frequency, 10 mW microwave power and 5 G modulation amplitude.

3. Results

3.1. HRP activity at pH 3.0

HRP solutions in water at pH 3.0 were prepared by adjusting their pH values with 2 N HCl and thus contained ~ 1 mM HCl. The enzyme dissolved in water at pH 3.0 was active, its activity being $500 \mu\text{mol product min}^{-1} (\text{mg enzyme})^{-1}$. This value corresponds to 50% of the activity measured at pH 6.5 in water (Table 1). In these experimental conditions (water pH 3.0) the enzyme was stable and, upon storage at 4°C , its activity kept constant for a week. At low pH, H_2PO_4^- was shown to affect HRP activity which decreased almost exponentially by increasing the concentration of dihydrogenphosphate (10–500 mM) (Table 1). The enzyme resulted completely inactive in the presence of 500 mM H_2PO_4^- and 40 mM Cl^- . The effect of Cl^- alone was investigated as well: 40 mM Cl^- induced a slight inactivation of HRP (68% of the activity measured in water pH 3.0), while total inactivation was obtained upon addition of 500 mM Cl^- and 20-min incubation.

3.2. Optical and binding measurements

The optical spectrum of HRP in water at pH 3.0 (Fig. 1b) was superimposable on those recorded at pH 6.5 in water (Fig. 1a) and in 10 mM phosphate buffer (data not shown): it was characterized by a Soret band at 403 nm and by two weaker absorptions at 500 and 640 nm. According to previously reported data [2], HRP Soret band appeared asymmetric due to a shoulder at 380 nm.

Cl^- and H_2PO_4^- brought about substantial modifications of HRP optical spectrum. Forty mM chloride induced an instantaneous Soret band red-shift (408 nm): this band became narrower and the shoulder at 380 nm was less evident. The charge-transfer bands were affected as well, one being red-shifted (500 \rightarrow 502 nm) and the other one being blue-shifted (640 \rightarrow 638 nm) (Fig. 1c and Table 2).

Incubation of the enzyme in the presence of 400 mM dihydrogenphosphate was responsible for a wider and

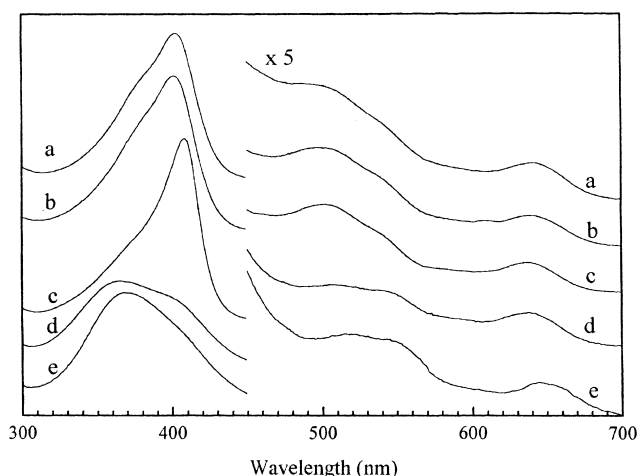


Fig. 1. HRP optical spectra: (a) pH 6.5 in water; (b) pH 3.0 in water; (c) like (b) + Cl^- 40 mM, (d) like (b) + H_2PO_4^- 400 mM, (e) like (b) + Cl^- 40 mM and H_2PO_4^- 400 mM.

blue-shifted Soret band (370 nm); the component at 403 nm was still evident (Fig. 1d). The corresponding modifications underwent by the charge-transfer bands are listed in Table 2. A further effect became evident when HRP was incubated in the presence of both anions: a clear-cut Soret band shifting to 370 nm took place and no absorption peak was left at 403 nm (Fig. 1e). This result is in agreement with a previous observation made by Smulevich et al. [21] in similar experimental conditions. Four hundred mM chloride was found to mimic the concerted effect of 400 mM dihydrogenphosphate + 40 mM chloride at pH 3.0 (data not shown).

Fig. 2 shows the binding curve for the HRP/chloride adduct; a $K_d = 9$ mM was extrapolated according to a previously reported method [22]. Its typical Michaelis-Menten pattern is indicative of an instantaneous interaction at a specific site. The interaction of dihydrogenphosphate with HRP resulted in a sigmoidal binding curve (Fig. 3b). A similar pattern (although less pronounced) resulted from binding of dihydrogenphosphate in the presence of saturating chloride concentration (40 mM \cong 4-fold K_d) (Fig. 3a). This pattern could arise from two different phenomena: either dihydrogenphosphate binds at $n \geq 2$ specific sites on

Table 1
HRP activity vs. H_2PO_4^- and Cl^- concentration in water

$[\text{H}_2\text{PO}_4^-]$ (mM)	$[\text{Cl}^-]$ (mM)		Activity ($\mu\text{mol product} \cdot \text{mg enzyme}^{-1} \cdot \text{min}^{-1}$)
–	–	pH 6.5	994
–	–	pH 3.0	500
10	–		499
50	–		496
125	–		359
300	–		301
500	–		247
–	40	pH 3.0	340
–	500 ^a		1.5
500	40	pH 3.0	0

^a After 20-min incubation.

Table 2
Optical spectra of HRP and its adducts in water at pH 3.0

Sample	Absorption (λ_{max} , nm)			
HRP	403	500	–	640
HRP- Cl^- ^a	408	502	–	638
HRP- Cl^- ^b	370	519	545 (sh)	651
HRP- H_2PO_4^-	370	510	545 (sh)	642
HRP- $\text{H}_2\text{PO}_4^-/\text{Cl}^-$	370	516	545 (sh)	644
HRP- $\text{H}_2\text{PO}_4^-/\text{Cl}^-$ ^c	370	519	546	652

^a $[\text{Cl}^-]$ 40 mM.

^b $[\text{Cl}^-]$ 500 mM.

^c Ref. [21].

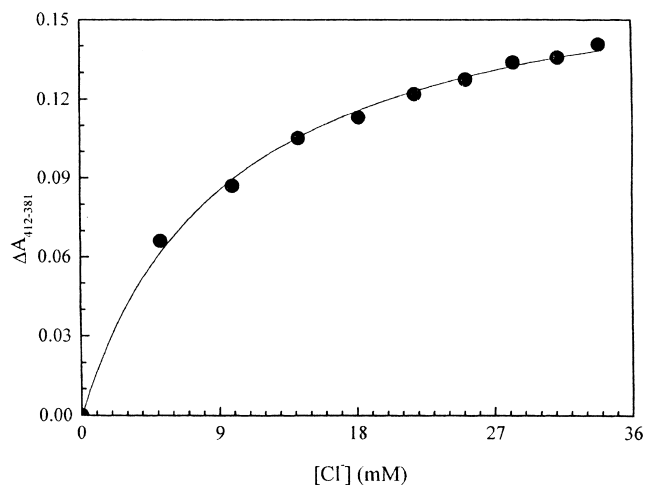


Fig. 2. Cl^- binding curve to HRP in water at pH 3.0.

the enzyme molecule or a kinetic effect (triggered by the interaction of H_2PO_4^- with the protein scaffold) takes place. Hill's coefficient was found to change when samples were incubated for different lengths of time (data not shown), before the measurement was started. This time-dependence supports the hypothesis of a kinetic effect. Hence, no K_d value for dihydrogenphosphate was extrapolated.

Fig. 4 reports the evolution of HRP optical spectrum upon addition of increasing concentrations of dihydrogenphosphate (0–400 mM) in the absence (a) or presence of 40 mM chloride (b), respectively. Fig. 4c shows the effect of increasing chloride concentrations (0–400 mM) on the same spectrum. The clear-cut isosbestic point shown in Fig. 4a indicates the presence of an equilibrium between two species; the more complex pattern shown in Fig. 4b and 4c, results from simultaneous equilibria

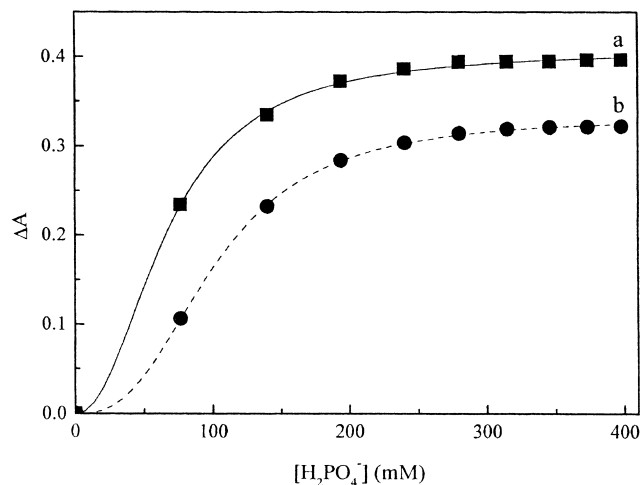


Fig. 3. H_2PO_4^- binding curves to HRP in water at pH 3.0 a) (■) in the presence of 40 mM Cl^- ($\Delta\text{Abs}_{404-409\text{ nm}}$); b) (●) in the absence of Cl^- ($\Delta\text{Abs}_{437-403\text{ nm}}$).

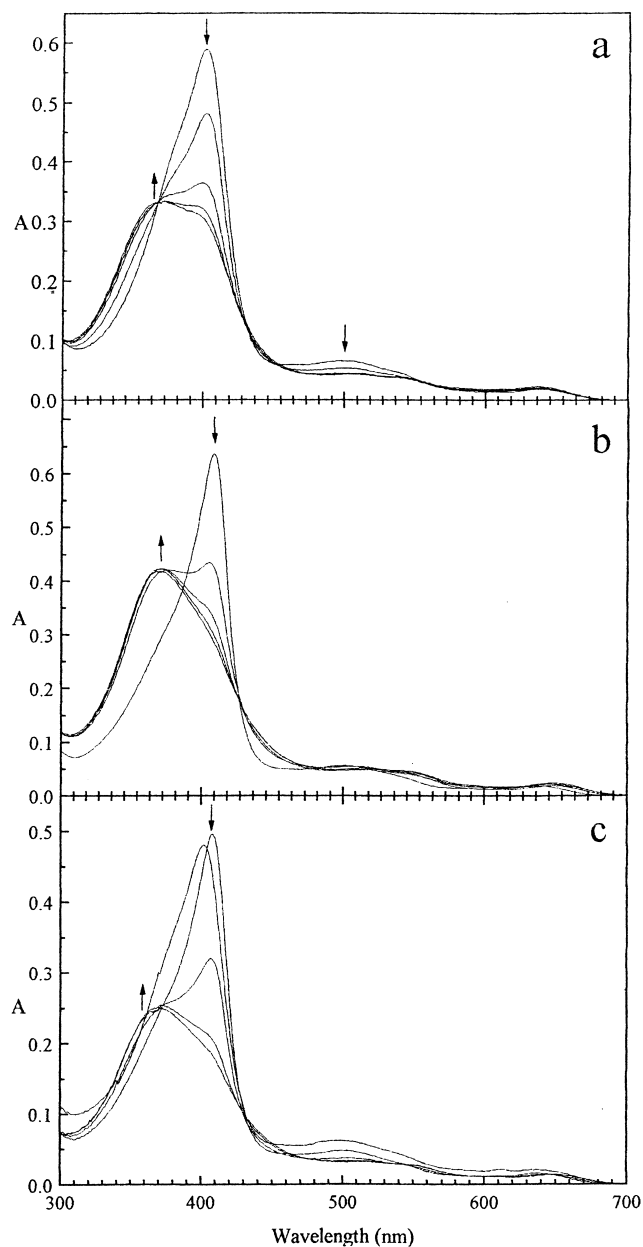


Fig. 4. Optical spectra of HRP in water at pH 3.0 in the presence of increasing amounts of: (a) H_2PO_4^- (0–400 mM); (b) H_2PO_4^- (0–400 mM) + 40 mM Cl^- ; (c) Cl^- (1–400 mM).

between, at least, three species. Shifting of the Soret band towards 370 nm was evident in all cases.

Finally, since a time-dependent effect of low pH on the optical spectrum of HRP has been reported [21] in the presence of high chloride and dihydrogenphosphate concentrations, we decided to carry out some further investigations, in order to clarify the role played by anions and ionic strength in modulating HRP structure and activity at low pH. We studied the evolution of the absorption at 403 nm vs. time, in the presence of 400 mM H_2PO_4^- and after addition of increasing chloride amounts (up to 400 mM) (Fig. 5). The absorbance at 403 nm

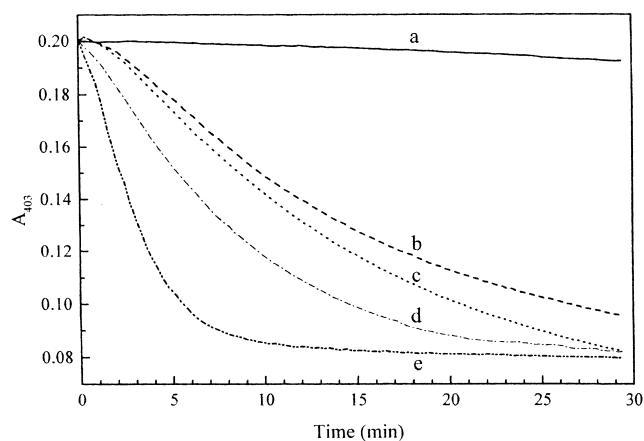


Fig. 5. $A_{403\text{ nm}}$ time-dependence for HRP in water at pH 3.0 in the presence of: (a) 40 mM Cl^- ; (b) 400 mM H_2PO_4^- ; (c) 400 mM H_2PO_4^- + 40 mM Cl^- ; (d) 400 mM Cl^- ; (e) 400 mM H_2PO_4^- + 400 mM Cl^- .

(Abs_{403}) decreased with time. The decay was slow in the absence of chloride (Fig. 5b). Addition of 40 mM Cl^- increased the decay rate (Fig. 5c), which became strikingly faster when 400 mM chloride was present (Fig. 5e). A similar decay, although slightly slower, was observed in the presence of 400 mM chloride only (in the total absence of dihydrogenphosphate) (Fig. 5d), while 40 mM Cl^- left Abs_{403} almost unchanged in a 30-min time-range (Fig. 5a).

3.3. EPR characterization

The EPR spectrum of HRP at pH 6.5 in 10 mM phosphate buffer (Fig. 6a) as well as in water pH 6.5 (data not shown) is characterized by a typical rhombic high-spin Fe(III) signal, with two absorptions in the g_{\perp} region ($g_x=6.3$ and $g_y=5.6$) and a weak band around $g_z=2$ (not shown), which has been interpreted as a quantum-mechanical admixture of high-spin ($S=5/2$) and intermediate-spin ($S=3/2$) states [6]. According to the literature, this spectral pattern does not change significantly in the pH range 4.5–7.0 [5,24].

The EPR spectral features of HRP at pH 3.0 in water looked changed (Fig. 6b): two strong additional absorptions became evident at $g_x=6.6$ and $g_y=5.3$. This spectrum could account for the presence of two species: a prevalent one, with a highly rhombic EPR pattern; a minor component, whose spectrum was similar to that recorded at neutral pH. The higher rhombicity component that prevails at low pH might be associated to the presence of a six-coordinate high-spin iron ion, with a water molecule (Wat92) as the axial ligand. This point will be discussed in more detail in the following section.

As dihydrogenphosphate has a striking effect on HRP optical pattern, we decided to investigate how it modifies the EPR features of the enzyme.

A series of EPR spectra of HRP were recorded in the

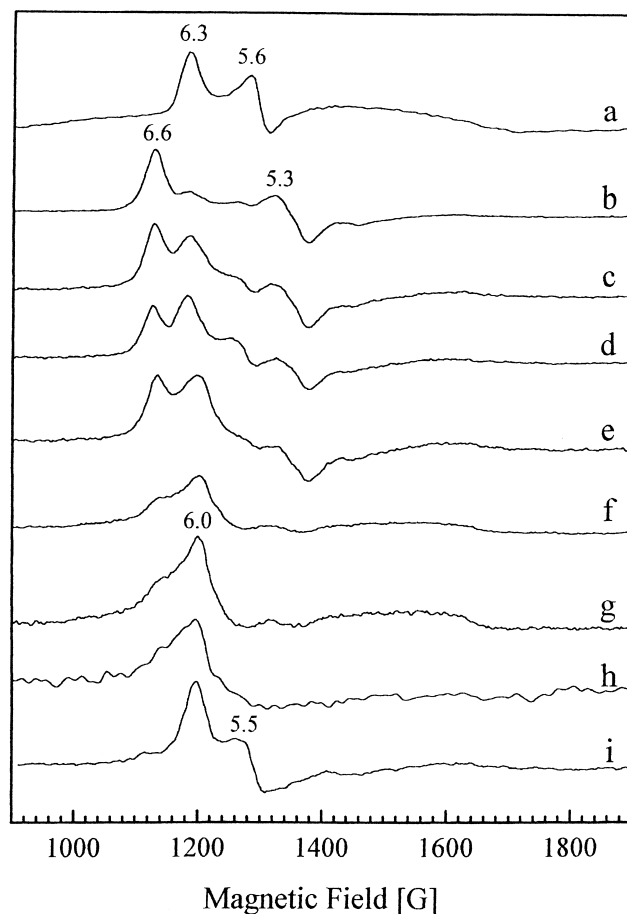


Fig. 6. Low temperature (4 K) EPR spectra of HRP in: (a) phosphate buffer 10 mM pH 6.5; (b) water pH 3.0; (c–g) water pH 3.0 + H_2PO_4^- 10 mM, 50 mM, 100 mM, 200 mM and 500 mM respectively; (h) water pH 3.0 + 40 mM Cl^- and 500 mM H_2PO_4^- ; (i) water pH 3.0 + 40 mM Cl^- .

presence of increasing H_2PO_4^- concentration (10–500 mM) (Fig. 6c–g). The $g_x=6.3$ and $g_y=5.6$ spectral components were increased by addition of 10 mM dihydrogenphosphate. Further additions resulted in a stronger $g=6.3$ absorption (which slowly shifted towards $g=6.0$), while the $g_x=6.6$ and $g_y=5.3$ bands slowly disappeared. Five hundred mM H_2PO_4^- resulted in a single EPR band at $g=6.0$ with apparent axial symmetry, although a residual contribution at lower field was still detectable (Fig. 6g). Addition of 40 mM chloride to this solution did not affect the spectrum significantly (Fig. 6h), although the low signal-to-noise ratio might hide a different size of the shoulder around $g=6.6$. Spectrum i) (which refers to HRP + 40 mM chloride, in the absence of dihydrogenphosphate) showed an apparent rhombic pattern (with two absorptions at $g_x=6.0$ and $g_y=5.5$) similar to that of native HRP at neutral pH, but characterized by lower rhombicity ($R\%=3.12$) and lower g_x value. A comparison between spectra g) and i) suggests that the unique EPR signal observed in the former coincides with the g_x absorption present in the latter one. Further addition of

chloride up to 500 mM did not change the EPR spectral pattern (data not shown).

4. Discussion

A peculiar characteristic of the HRP structure consists of an extensive H-bonds network, which accounts for the high flexibility of its structure and for its sensitivity to pH. Any factor able to perturb the H-bond network may influence the protein conformation, the Fe(III)-heme environment and the stability of the Fe(III)-imidazolate bond on the proximal side of the heme pocket; as a consequence, the protein spectral features would be affected. Most of our experimental data have been interpreted in the light of this assumption. A schematic representation of the hypothesized coordination structures of HRP at pH 3.0 (and at pH 6.5) in water, in the presence of chloride and dihydrogenphosphate is given in Fig. 7.

HRP at pH 3.0 retains 50% activity compared to pH 6.5

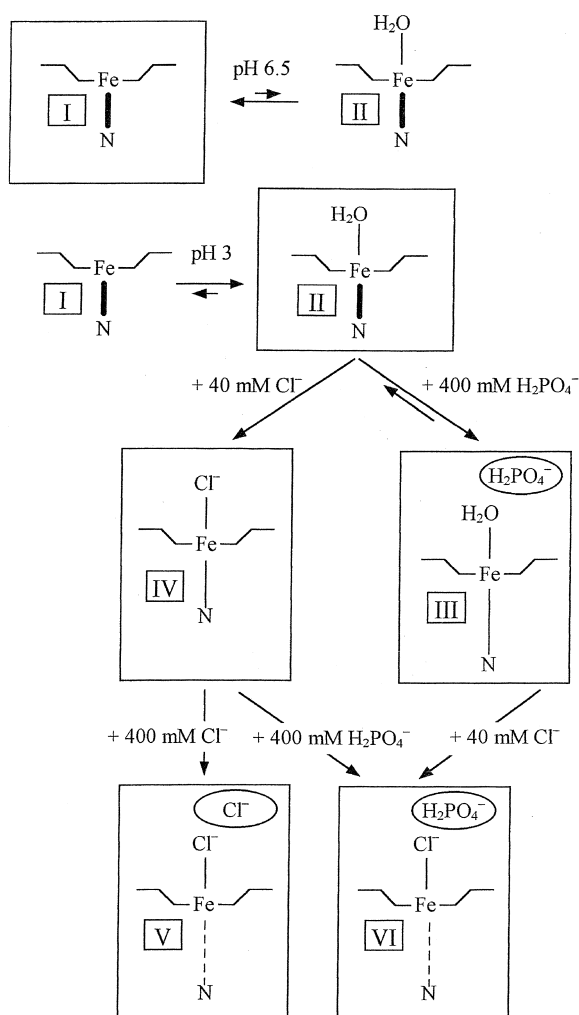


Fig. 7. Mechanistic model showing the effects of low pH, ionic strength, Cl⁻ and H₂PO₄⁻ on HRP catalytic site.

(Table 1). Low pH does not seem to affect the catalytic activity with time, since it kept constant for a week. The optical spectrum is unchanged with respect to neutral pH (Fig. 1). Nonetheless a modification of HRP conformation is suggested by our EPR data, which are consistent with the presence of two species of different rhombicity (Fig. 6).

X-ray data on rHRPc show that a water molecule (Wat92) lies at 3.2 Å from the iron, in the distal region of HRP catalytic pocket. Moreover, binding of benzhydroxamic acid perturbs the H-bond network and induces Wat92 to move towards the iron ion (2.6 Å) [10,11]. Smulevich et al. [12] suggest that HRP at neutral pH might undergo an equilibrium between two forms: a prevalent one, which is characterized by a 5-coordinated heme-iron (I, Fig. 7); a very minor one, with a 6-coordinated iron ion (II Fig. 7), the sixth ligand being Wat92. Shifting of this equilibrium is expected to affect the EPR features of HRP, since it implies a net change in the coordination geometry of iron [12]. Our EPR data indicates that pH influences this equilibrium, by inducing a conformational shift towards the 6-coordinated form of the enzyme. The EPR spectrum of HRP at pH 3.0 results from the superposition of two distinct spectral patterns: a minor one, that we assign to the 5-coordinated form prevailing at neutral pH ($g_x=6.3$ and $g_y=5.6$; $R\%=4.37$); a major component, which is characterized by higher rhombicity ($g_x=6.6$ and $g_y=5.3$; $R\%=8.12$) and is associated with the 6-coordinated form of HRP, whose amount is negligible at neutral pH.

On the other hand, being H₂O a weak ligand, the optical spectrum is not expected to be strongly perturbed as a result of water coordination. It is worth to remind that apparent discrepancies between optical and EPR data are related to the different temperature at which they are recorded: 4 K for EPR and room temperature for UV-Vis spectroscopy. Dynamic equilibria existing at RT are obviously blocked when temperature is lowered. Thus, the two situations are not coincident and they may be not easily comparable. On the other hand, being EPR specifically sensitive to changes of the coordination symmetry while optical data are influenced by perturbations of the energetic state of the metal center brought about by ligand binding, we think that the concerted use of EPR and optical spectroscopy may provide complementary and useful information on the properties of the system.

The conformational modification underwent by HRP at pH 3.0 can be correlated to a perturbation of the H-bonds network. The central role of this network in stabilizing the active conformation of HRP, by coupling the protein domains lying above and below the heme plane has already been stressed [10]. Lowering of pH induces protonation of the distal histidine N_ε (His42) and may relax the hydrogen network inside the catalytic pocket. This could induce a conformational rearrangement allowing Wat92 (the water molecule closest to the iron) to coordinate to the metal. This is expected to modulate heme

accessibility to substrates and inorganic anions. Our experimental data show that a peculiar interaction of HRP with chloride and dihydrogenphosphate takes place at pH 3.0 (Figs. 1, 6) but it is not observed at pH 6.5. These experimental observations fit the change in Wat92 localization.

EPR (Fig. 6) and optical (Fig. 1, Table 2) data *inequivocally* indicate that chloride binds directly to the iron site and replaces the water molecule in the axial position (IV Fig. 7). Although hexacoordination is maintained upon chloride binding, the overall perturbation induced by Cl^- on the H-bonding network is lower. Such effect will be further discussed in relationship to the perturbation induced by dihydrogenphosphate. At pH 3.0 in the presence of 40 mM Cl^- , the HRP/ Cl^- adduct is stable and its K_d value (Fig. 2) is comparable to those reported for similar adducts of HRP with anionic ligands [25,26]. The process is not time-dependent; formation of a 6-coordinated species is supported by the clear-cut Soret band shift to 408 nm as well as by the blue-shift of the CT1 band (640→638 nm), in agreement with previously published data [13]. HRP in the presence of 40 mM Cl^- is still active: this shows that the Fe-His bond is not broken.

A more complex situation was observed for H_2PO_4^- (pH 3.0). Both EPR (Fig. 6) and optical (Fig. 1, 4a, Table 2) spectra, as well as binding data (Fig. 3b), are consistent with the presence of a slow equilibrium between species II and III in Fig. 7 (which is also suggested by the time-dependent decay of Abs_{403} , Fig. 5b). H_2PO_4^- may bind at any accessible cationic site, inside or outside the heme pocket. Inside the active site, positively charged aminoacids like Arg31 or Arg38 [10] might be involved in this interaction. One should remember that Arg38 is a crucial residue of HRP H-bonds' network. Hence, binding at this site may perturb protein conformation. On the other hand, dihydrogenphosphate may interact with any cationic site exposed to the solvent and this is expected to result in a conformational rearrangement of the protein scaffold, related to a change of charge-distribution over the enzyme surface. Such a process is expected to be time-dependent.

Met-Mb has been shown to undergo a conformational transition, triggered by low pH [27]. The time-dependent modification of its optical spectrum, ending up with the appearance of a band at 370 nm was taken as an evidence for such an event. This absorption was associated with a 'partially unfolded' form of the protein. The time-dependent evolution of HRP Soret absorption in the presence of H_2PO_4^- (Fig. 5b, c), the sigmoidal pattern of dihydrogenphosphate binding curves and the appearance of an optical band at 370 nm strongly suggest that a similar phenomenon takes place in HRP. Further we notice that 500 mM H_2PO_4^- does not induce breakage of the Fe-His bond, since the enzyme retains 25% activity compared to pH 6.5 (Table 1).

In the light of these results, we attempted to address the question if such an effect was specifically due to dihydro-

genphosphate or rather related to high ionic strength (since it took place exclusively in the presence of high anion concentration), independently from the nature of the ion involved.

Addition of 40 mM chloride to an HRP solution containing 400 mM H_2PO_4^- modifies the equilibrium balance: species VI (Fig. 7) is generated, whose optical spectrum (Figs. 1, 4b) reminds the one reported by Smulevich et al. in similar experimental conditions [21] as indicative of the Fe-His bond breakage (acid transition). At the same time, spectral features assigned to species II have disappeared. An exclusive dependence of this conformational equilibrium on low pH conditions was claimed [21], while no ionic strength influence was considered. In the light of our results, we suggest that, although low pH is required to bring about this modification, the crucial factor is ionic strength. Therefore, analogous measurements were made in the presence of 500 mM chloride concentration (and no dihydrogenphosphate). The optical data (Figs. 1, 4c, 5d) show that, in this case, a situation similar to the one induced by 400 mM H_2PO_4^- /40 mM Cl^- is observed, as witnessed by the Soret band shift from 408 nm to 370 nm (Fig. 4b,c). Thus the HRP/ Cl^- adduct is formed first, followed by a conformational transition of the enzyme caused by ionic strength (400 mM chloride or dihydrogenphosphate). In other words, the specific binding of chloride to the iron gives reason for the Soret band red-shift; the diffused interaction of either chloride or dihydrogenphosphate with the protein induces the blue-shift to 370 nm. In conclusion, the sum of an unspecific and a specific interaction is observed in the presence of chloride and high ionic strength, which result in formation of species V and VI (Fig. 7).

We suggest that replacement of Wat92 by Cl^- as the sixth ligand (IV Fig. 7) together with a conformational rearrangement of the heme pocket (induced by ionic strength) accounts for the modified EPR spectral pattern as well as for a weakening of the Fe(III)-imidazolate bond; as soon as ionic strength increases, this bond breaks (V and VI Fig. 7) giving rise to a 5-coordinated species. This is in agreement with our activity measurements: although dihydrogenphosphate induces a strong decrease of enzyme activity, HRP inactivation takes place only in the presence of 40 mM Cl^- + 500 mM H_2PO_4^- (or, alternatively, 500 mM Cl^-). Such a process (related to the non-specific effect displayed by these anions) is not instantaneous (Fig. 5); a 20 min delay is required to let the system reach the equilibrium. The sigmoidal pattern of the dihydrogenphosphate binding curve (Fig. 3b) as well as the A_{403} decay (Fig. 5) originate from this phenomenon.

The difference in size of the chloride and dihydrogenphosphate ions may explain the discrepancy between EPR spectral patterns recorded in the presence of 500 mM Cl^- or 40 mM chloride/500 mM dihydrogenphosphate, respectively. We suggest that the bulky ion dihydrogenphosphate is able to induce distortions in the heme-pocket

geometry, resulting in an almost axial EPR signal. On the contrary, chloride being relatively small, it cannot exert significant constraints and leaves the active-site geometry almost undistorted.

Low pH has already been reported to induce acid transitions in hemoproteins [21,24,27–29], involving breaking of the Fe-imidazolate bond on the proximal side of the heme pocket. Polizio et al. [30] reports that acid transition in nitrosylated Mb occurs at pH 4.5 exclusively in the presence of phosphate ions: low pH cannot induce breaking of the Fe–N bond, unless 0.2 M phosphate is present. This seems to be the case of HRP as well, although dihydrogenphosphate plays the unique role of raising ionic strength and can be replaced by chloride.

Chloride, ionic strength and low pH appears to act synergistically in order to bring about a transition from an axial 6-coordinated symmetry (due either to chloride or water binding to the iron, II and IV in Fig. 7) to a 5-coordinated rhombic geometry (due to breaking of the Fe–N bond, V and VI Fig. 7). These three factors separately modulate equilibria between species II, III, IV, V and VI (Fig. 7) but a net shift towards species V and VI is achieved only as a result of their concerted effect.

A description of the synergistic effect played by chloride, ionic strength and low pH in modulating HRP conformation is given in this paper. Modifications of HRP spectral properties in the presence of chloride at pH 3.0 and high ionic strength conditions have been observed. Their correlation to a change of the Fe(III) coordination sphere (due to water replacement by chloride) as well as of the extensive H-bond network which bridges the distal and proximal side of the enzyme has been discussed.

5. Abbreviations

HRP	Horseradish Peroxidase
rHRPc	Isoenzyme C of recombinant HRP
Mb	Myoglobin
EPR	Electron Paramagnetic Resonance
R%	Apparent rhombicity

Acknowledgements

Support from the Italian Ministero per l'Università e la Ricerca scientifica e Tecnologica (MURST) [PRIN 1998-prot. 9803184222] and from Consiglio Nazionale delle Ricerche (CNR) is kindly acknowledged.

References

- [1] H. Kohler, H. Jenzer, *Free Rad. Biol. Med.* 6 (1989) 323–339.
- [2] H.B. Dunford, J.S. Stillman, *Coord. Chem. Rev.* 19 (1976) 187–251.
- [3] J.H. Dawson, *Science* 240 (1988) 433–439.
- [4] H.B. Dunford, D. Job, *Eur. J. Biochem.* 66 (1976) 607–614.
- [5] M. Tamura, H. Hori, *Biochim. Biophys. Acta* 284 (1972) 20–29.
- [6] M.M. Maltempo, P.I. Ohlsson, K.G. Paul, L. Petersson, A. Ehrenberg, *Biochemistry* 18 (1979) 2935–2941.
- [7] C.E. Schulz, R. Rutter, J.T. Sage, P.G. Debrunner, L.P. Hager, *Biochemistry* 23 (1984) 4743–4754.
- [8] J. Huang, H.B. Dunford, *Can. J. Chem.* 68 (1990) 2159–2163.
- [9] M.A. Ator, P.R. Ortiz de Montellano, *J. Biol. Chem.* 262 (1987) 1542–1551.
- [10] M. Gajhede, D.J. Schuller, A. Henriksen, A.T. Smith, T.L. Poulos, *Nat. Struct. Biol.* 4 (1997) 1032–1038.
- [11] A. Henriksen, D.J. Schuller, K. Meno, K.G. Welinder, T.A. Smith, M. Gajhede, *Biochemistry* 37 (1998) 8054–8060.
- [12] G. Smulevich, M. Paoli, J.F. Burke, S.A. Sanders, N.F. Roger, *Biochemistry* 33 (1994) 7398–7407.
- [13] B.D. Howes, J.N. Rodriguez-Lopez, A.T. Smith, G. Smulevich, *Biochemistry* 36 (1997) 1532–1543.
- [14] J.N. Rodriguez-Lopez, A.T. Smith, R.N.F. Thorneley, *J. Biol. Inorg. Chem.* 1 (1996) 136–142.
- [15] L. Banci, P. Carloni, G. Gori Savellini, *Biochemistry* 33 (1994) 12356–12366.
- [16] R.H. Haschke, J.M. Friedhoff, *Biochem. Biophys. Res. Comm.* 80 (1978) 1039–1042.
- [17] Y. Shiro, M. Kurono, I. Morishima, *J. Biol. Chem.* 261 (1986) 9382–9390.
- [18] R.P. Ferrari, E. Laurenti, M. Rossi, *Life Chem. Rep.* 10 (1994) 249–258.
- [19] R. Roman, H.B. Dunford, *Biochemistry* 11 (1972) 2076–2082.
- [20] T.K. Das, S. Mazumdar, *Eur. J. Biochem.* 227 (1995) 823–828.
- [21] G. Smulevich, M. Paoli, G. De Sanctis, A.R. Mantini, F. Ascoli, M. Coletta, *Biochemistry* 36 (1997) 640–649.
- [22] R.P. Ferrari, S. Traversa, L. De Gioia, P. Fantucci, G. Suriano, E.M. Ghibaudi, *J. Biol. Inorg. Chem.* 4 (1999) 12–20.
- [23] R.P. Ferrari, E.M. Ghibaudi, S. Traversa, E. Laurenti, L. De Gioia, M. Salmona, *J. Inorg. Biochem.* 68 (1997) 17–26.
- [24] W.E. Blumberg, J. Peisach, A. Wittenberg, J.B. Wittenberg, *J. Biol. Chem.* 243 (1968) 1854–1862.
- [25] S. Modi, D.V. Behere, S. Mitra, *J. Biol. Chem.* 264 (1989) 19677–19684.
- [26] J. Sakurada, S. Takahashi, T. Hosoya, *J. Biol. Chem.* 262 (1987) 4007–4010.
- [27] V. Palaniappan, D.F. Bocian, *Biochemistry* 33 (1994) 14264–14274.
- [28] F. Yang, G.N. Phillips, *J. Mol. Biol.* 256 (1996) 762–774.
- [29] P. Ascenzi, M. Brunori, M. Coletta, A. Desideri, *Biochem. J.* 258 (1989) 473–478.
- [30] F. Polizio, G. De Sanctis, P. Ascenzi, M. Coletta, *J. Biol. Inorg. Chem.* 3 (1998) 458–462.